Reviews

Stereoselective effects, formation thermodynamics, substitution reaction kinetics, and structures of transition metal complexes with bioligands and aromatic N-donors*

V. G. Shtyrlin,★ N. Yu. Serov, M. S. Bukharov, E. M. Gilyazetdinov, M. A. Zhernakov, M. A. Ahmed, A. R. Garifzyanov, I. I. Mirzayanov, A. V. Ermolaev, N. S. Aksenin, K. V. Urazaeva, and A. V. Zakharov

A. M. Butlerov Chemical Institute, Kazan Federal University, 18 ul. Kremlevskaya, 420008 Kazan, Russian Federation.

Fax: +7 (843) 238 7901. E-mail: Valery.Shtyrlin@gmail.com

A brief review presents the results obtained by our research team in recent years on the structures (in the solid state and in solution), thermodynamics, stereoselectivity of the formation, and the kinetics of substitution reactions for a number of homo- and mixed-ligand complexes of some 3d elements with enantiomerically homogeneous and racemic forms of amino acids, natural di- and tripeptides, aromatic N-donors, new phosphorylated dithiocarbamates and hydrazone derivatives at different salt concentrations at several temperatures. Reliable results were obtained using spectroscopic methods, including spectrophotometry, EPR, and NMR relaxation, X-ray diffraction analysis, the stopped-flow method with spectrophotometric detection, and pH-metry in combination with mathematical modeling using a number of modern, including our own, programs. The structures of the complexes in solution were characterized by DFT quantum chemical calculations and molecular dynamics simulations. The key factors controlling the stereoselectivity of the complex formation, the stability of complexes, and the kinetics of ligand substitution reactions were revealed.

Key words: coordination compounds, thermodynamics, kinetics, structure, stereoselectivity, spectroscopic methods, quantum chemistry.

The elucidation of the factors responsible for the specificity and selectivity of processes in the living nature and related biological activity of compounds is a challenge in modern science. Investigations in the field of coordination and bioinorganic chemistry can make a significant contribution to solving this problem. To that end, this authors' review presents

* Based on the materials of the XIX International Conference "Spectroscopy of Coordination Compounds" (September 18—23, 2022, Tuapse, Russia).

Published in Russian in *Izvestiya Akademii Nauk. Seriya Khimicheskaya,* Vol. 72, No. 7, pp. 1485—1498, July, 2023.

1066-5285/23/7207-1485

the most important results obtained by our research team in recent years on the structures, thermodynamics, stereoselectivity of the formation, and kinetics of substitution reactions for a number of homo- and mixed-ligand complexes of 3d elements with amino acids with different chirality, natural di- and tripeptides, aromatic N-donor ligands, phosphorylated dithiocarbamates, and new hydrazone derivatives at different salt concentrations at 25.0 and 37.0 °C.[1] Reliable results were obtained using complementary spectroscopic methods, the stopped-flow spectrophotometric method, and pH-metry. Mathematical modeling methods using modern programs, including the authors' programs STALABS[2] and STALABS-M,[3] were widely applied in the calculations. The structures of many complexes in solution were determined by DFT quantum chemical calculations and molecular dynamics (MD) simulations.

Special mention should be made on the methods of obtaining reliable data on the complexation in solution and the solid state. The pH potentiometry is the most consistent and robust technique for investigating the complexation. Whenever possible, one should start investigations with this technique followed by the use of spectroscopic, quantum chemical, and other methods to study the structures, thermodynamics of formation, and kinetics of substitution reactions and ligand exchange in homo- and mixed-ligand complexes.

Let us consider the factors responsible for the specificity and selectivity of the complexation of metals with enantiomerically homogeneous and racemic forms of ligands of different nature.

Nickel(II)—L/DL-histidine (HisH) systems provide a bright example of the stereoselectivity.[3] Table 1 presents the formation constants of binary complexes in these systems calculated from the results of pH-metric titration and spectrophotometry (SP-metry). The stereoselectivity of the complexation is evaluated from the difference between the logarithms of the formation constants of the complexes (Δlogβ) and is considered as statistically significant when the value of Δlogβ is larger than twice the sum of the standard deviations of each constant to be compared (these deviations in the last digit are given in parentheses). As can be seen in Table 1, the bis- and tris-complexes $[Ni(His)(HisH)]^+$, $Ni(His)_2$, $[Ni(His)(HisH_{-1})]^-$, and $[Ni(His)_3]^-$ satisfy the condition of significant stereoselectivity, the *meso* forms (forms with enantiomerically different ligands) being predominant for the last three complexes.

The experimental data on the enantioselectivity are consistent in detail with the results of quantum chemical calculations. Hereinafter, the calculations were performed using the GAMESS[4] and ORCA programs[5] by the DFT method[6] with the exchange-correlation functionals B3LYP[7,8] and CAM-B3LYP[9] using the TZVP basis set[10] and also at the PBE/TZVPP level of theory[11] with the inclusion of the solvent effects taking into account the polarizable continuum model C-PCM.[12] In all calculations, the local energy minima were determined with the acceptance criterion of 10^{-5} a.u. As can be seen in Fig. 1, the formation of the DL form (*meso* form) is preferable for nickel(II) bis-histidinate. However, the *meso* form was found to be energetically less favorable than

Table 1. Logarithms of the formation constants (logβ) for nickel(II) complexes with L/DL-HisH (25.0 °C, 1.0 *M* KNO_3, $\Delta\log\beta = \log\beta_L - \log\beta_{DL}$)[3]

Equilibrium	logβ		Δlogβ
	L-His	DL-His	
$H^+ + His^- \rightleftharpoons HisH$	9.200(3)	—	—
$H^+ + HisH \rightleftharpoons [HisH_2]^+$	6.265(1)	—	—
$H^+ + HisH_2^+ \rightleftharpoons [HisH_3]^{2+}$	1.986(1)	—	—
$Ni^{2+} + HisH \rightleftharpoons [Ni(HisH)]^{2+}$	2.788(4)	2.791(3)	−0.003
$Ni^{2+} + His^- \rightleftharpoons [Ni(His)]^+$	8.576(1)	8.572(1)	0.004
$Ni^{2+} + His^- + HisH \rightleftharpoons [Ni(His)(HisH)]^+$	10.781(5)	10.757(4)	*0.024*
$Ni^{2+} + 2\ His^- \rightleftharpoons Ni(His)_2$	15.464(1)	15.707(1)	*−0.243*
$Ni^{2+} + 2\ His^- \rightleftharpoons [Ni(His)(HisH_{-1})]^- + H^+$	2.36(1)	2.62(1)	*−0.26*
$Ni^{2+} + 3\ His^- \rightleftharpoons [Ni(His)_3]^-$	15.77(1)	16.20(1)	*−0.43*

Note. Here and in Tables 2—12, the standard deviations in the last digit are given in parentheses; statistically significant differences in the constants that refer to enantiomerically different forms of the ligands are given in italic.

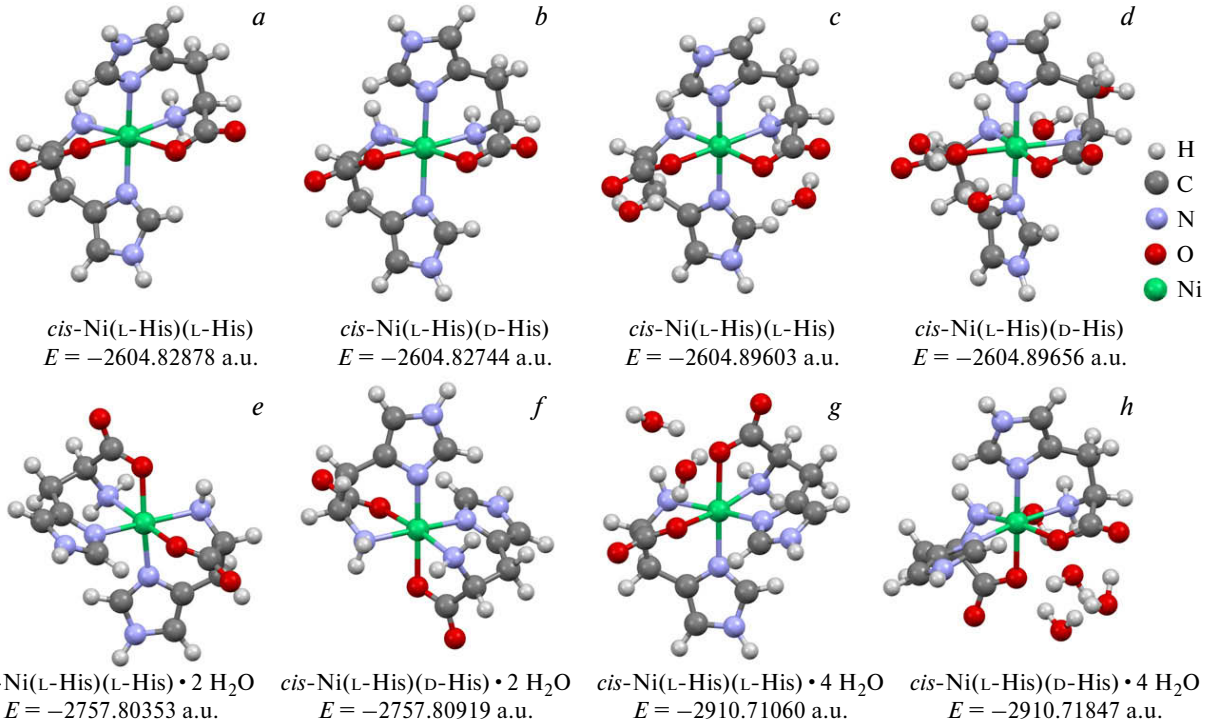

Fig. 1. Structures and formation energies of the most favorable isomers of the complexes $Ni(His)_2 \cdot nH_2O$ (n = 0, 2, 4) with ligands in different enantiomeric forms optimized at the CAM-B3LYP/TZVP level of theory in vacuum (*a*, *b*) and taking into account the solvent effects by the C-PCM model (*c*—*h*).[3]

the LL form in the calculations in vacuum and only without taking into account water molecules in terms of a discrete model. The reasons for this phenomenon deserve attention. The *cis* arrangement of identical groups of adjacent ligands is favored by the *trans* effect, resulting in that strong *trans*-directing ligands avoid being mutually *trans*. However, in the case of the *trans* arrangement of bulky imidazole groups in the LL form, the steric repulsion between them is diminished. If the *trans* effect competes with the steric effect, the solvation effect can make a decisive contribution. Actually, the *cis* structure of the *meso* form has a large dipole moment, thereby facilitating its solvation by water dipoles. As can be seen in Fig. 1,

Table 2. Logarithms of the formation constants (logβ) in nickel(II)—L/D-HisH—L-amino acid systems ($AspH_2$, $GluH_2$, SerH, MetH) (25.0 °C, 1.0 *M* KNO_3)

Equilibrium	Amino acid residues	logβ	Δlogβ
$Ni^{2+} + HisH + Asp^{2-} \rightleftharpoons Ni(HisH)(Asp)$	L-Asp, L-His	10.08(3)	
	L-Asp, D-His	10.19(3)	−0.11
$Ni^{2+} + His^{-} + Asp^{2-} \rightleftharpoons [Ni(His)(Asp)]^{-}$	L-Asp, L-His	14.319(5)	
	L-Asp, D-His	14.378(6)	*−0.059*
$Ni^{2+} + HisH + Glu^{2-} \rightleftharpoons Ni(HisH)(Glu)$	L-Glu, L-His	9.90(6)	
	L-Glu, D-His	10.03(4)	−0.13
$Ni^{2+} + His^{-} + Glu^{2-} \rightleftharpoons [Ni(His)(Glu)]^{-}$	L-Glu, L-His	13.28(1)	
	L-Glu, D-His	13.28(1)	0.00
$Ni^{2+} + His^{-} + Ser^{-} \rightleftharpoons Ni(His)(Ser)$	L-Ser, L-His	13.117(6)	
	L-Ser, D-His	13.111(7)	0.006
$Ni^{2+} + Ser^{-} + His^{-} \rightleftharpoons [Ni(His)(SerH_{-1})]^{-} + H^{+}$	L-Ser, L-His	1.776(8)	
	L-Ser, D-His	1.908(8)	*−0.132*
$Ni^{2+} + HisH + Met^{-} \rightleftharpoons [Ni(HisH)(Met)]^{+}$	L-Met, L-His	9.13(3)	
	L-Met, D-His	9.11(2)	0.02
$Ni^{2+} + His^{-} + Met^{-} \rightleftharpoons Ni(His)(Met)$	L-Met, L-His	13.079(6)	
	L-Met, D-His	13.166(5)	*−0.087*

Table 3. Thermodynamic parameters of the complexation in the nickel(II)—L-HisH—L/D-MetH system (25.0 °C, 1.0 *M* KNO_3)[3]

Equilibrium	logβ	$\Delta_r G°$	$\Delta_r H°$	$\Delta_r S°$/J (K mol)$^{-1}$
		kJ mol^{-1}		
Ni^{2+} + L-His^- ⇌ [Ni(L-His)]$^+$	8.576±0.001	−48.92±0.01	−31.40±0.34	58.8±1.1
Ni^{2+} + 2 L-His^- ⇌ $Ni(L\text{-}His)_2$	15.464±0.001	−88.19±0.01	−65.84±0.27	74.9±0.9
Ni^{2+} + L/DL-Met^- ⇌ [Ni(L/DL-Met)]$^+$	5.305±0.001	−30.37±0.01	−13.80±0.95	55.6±3.2
Ni^{2+} + 2 L/DL-Met^- ⇌ $Ni(L/DL\text{-}Met)_2$	9.855±0.001	−56.11±0.01	−33.09±0.54	77.2±1.8
Ni^{2+} + L-His^- + L-Met^- ⇌ Ni(L-His)(L-Met)	13.079±0.006	−74.66±0.03	−49.64±0.72	*83.9±2.4*
Ni^{2+} + L-His^- + D-Met^- ⇌ Ni(L-His)(D-Met)	*13.166±0.005*	−75.17±0.03	*−51.42±0.57*	79.7±1.9

the difference in the energy of formation of the above isomers increases with increasing number of water molecules introduced into their environment.

As follows from Table 2, there is significant stereoselectivity of the formation of mixed-ligand nickel(II) complexes with the histidinate anion, on the one hand, and aspartate (Asp^{2-}), serinate ($SerH_{-1}^{2-}$) with the deprotonated alcoholic group, and methioninate (Met^-), on the other hand. In all three cases, the *meso* forms are the major structures. This fact is consistent with the tridentate coordination of the mentioned amino acid anions as opposed to the bidentate coordination of glutamate (Glu^{2-}). The predominance of the *meso* form is confirmed by quantum chemical calculations.

Paradoxically, the stereoselectivity of the formation is not manifested in homoligand nickel(II) complexes with methionine, but it was observed for mixed-ligand complexes.[3] As can be seen in Table 3, the calorimetry studies showed that this effect is enthalpic in nature. According to the quantum chemical calculations (Fig. 2), there is a new type of weak interactions between the thiomethyl and imidazole groups in this complex, which is facilitated by the coordination of a sulfur atom to the metal.[3] It is worth noting that the new type of weak interactions found in our studies can be manifested in biological systems. In general, it can be concluded that the stereoselective preference of the *meso* forms of both homo- and mixed-ligand nickel(II) complexes

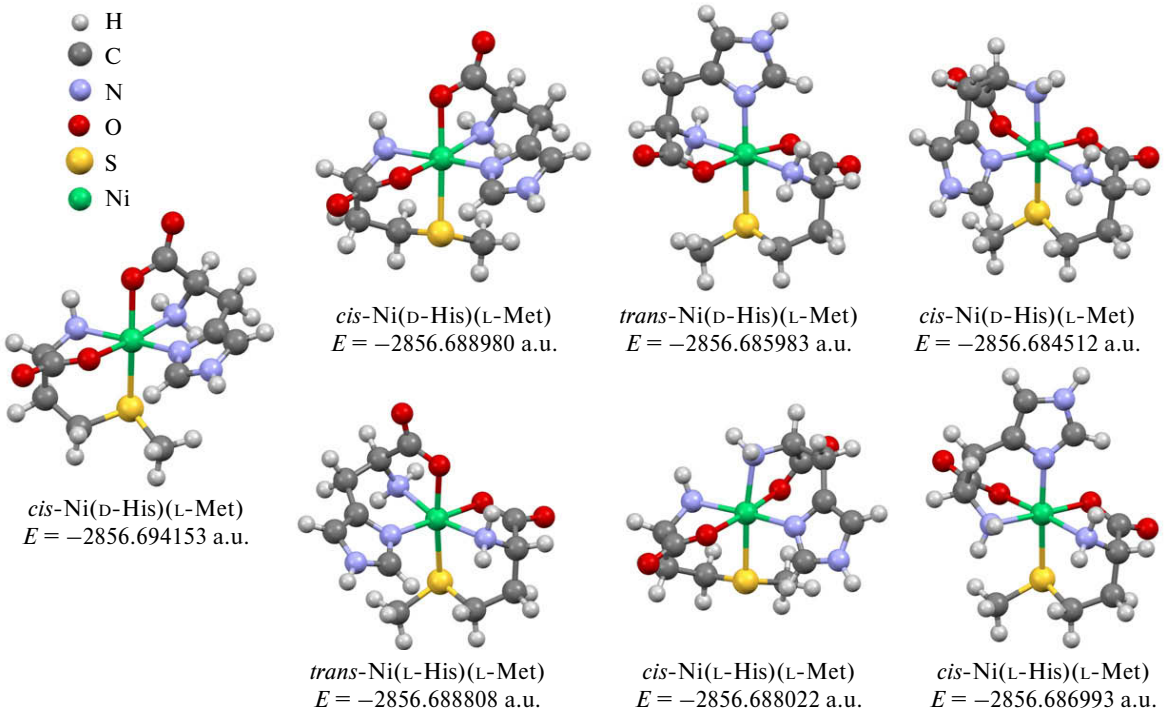

Fig. 2. Structures and formation energies of the possible isomers of the complexes Ni(His)(Met) with ligands in different enantiomeric forms optimized at the CAM-B3LYP/TZVP level of theory taking into account the solvent effects by the C-PCM model.[3]

Table 4. Logarithms of the formation constants (logβ) for homoligand zinc(II) complexes with L/DL-amino acids (HisH, MetH, PheH, TrpH) (25.0 °C, 1.0 *M* KNO_3)

Equilibrium	logβ		Δlogβ
	L	DL	
$Zn^{2+} + HisH \rightleftharpoons [Zn(HisH)]^{2+}$	2.250(2)	2.250(3)	0.000
$Zn^{2+} + His^- \rightleftharpoons [Zn(His)]^+$	6.466(1)	6.462(1)	0.004
$Zn^{2+} + His^- + HisH \rightleftharpoons [Zn(His)(HisH)]^+$	8.509(2)	8.499(2)	0.010
$Zn^{2+} + 2\ His^- \rightleftharpoons Zn(His)_2$	12.026(1)	12.143(1)	*−0.117*
$Zn^{2+} + 2\ His^- \rightleftharpoons [Zn(His)_2H_{-1}]^- + H^+$	1.336(6)	1.35(1)	−0.014
$Zn^{2+} + Met^- \rightleftharpoons [Zn(Met)]^+$	4.373(2)	4.373(3)	0.000
$Zn^{2+} + 2\ Met^- \rightleftharpoons Zn(Met)_2$	8.180(2)	8.174(5)	0.006
$Zn^{2+} + Phe^- \rightleftharpoons [Zn(Phe)]^+$	4.205(3)	4.202(3)	0.003
$Zn^{2+} + 2\ Phe^- \rightleftharpoons Zn(Phe)_2$	8.162(3)	8.222(2)	*−0.060*
$Zn^{2+} + Trp^- \rightleftharpoons [Zn(Trp)]^+$	4.38(1)	4.39(2)	0.010
$Zn^{2+} + 2\ Trp^- \rightleftharpoons Zn(Trp)_2$	8.751(4)	8.866(4)	*−0.115*

with amino acids is consistent with the manifestation of the *trans* effect combined with the effects of hydration and interligand interactions in complexes with *cis*-coordinated ligands.

The data on the complex formation of zinc(II) with amino acids[13,14] are interesting in terms of comparison with the nickel(II) complexes. It can be seen in Table 4 that, as in the case of nickel(II), the significant stereoselectivity is manifested in the formation of the homoligand complex $Zn(His)_2$ (through a d—π interaction) and the bis-complexes with phenylalanine (PheH) and tryptophan (TrpH), which is attributed to interligand π—π stacking interactions. Both these types of interactions occur in the *meso* forms.

The significant stereoselectivity is manifested in the formation of mixed-ligand complexes containing, apart from histidine, cysteine (CysH), phenylalanine, and tryptophan (Table 5). The latter two aromatic ligands can be involved in π—π stacking interactions with the coordinated imidazole group exactly in the *meso* forms. It should be noted that, unlike the nickel(II) complexes, the zinc(II) complexes favor the pseudotetrahedral coordination.

The data on the formation of complexes involving copper(II) are of great interest. The five-coordinate state of copper(II) in complexes with bioligands in aqueous solutions, which was discovered in our studies,[15,16] is an important factor responsible for the stereoselectivity of their formation and reactivity. We established this phenomenon based on the EPR and NMR water proton relaxation data and the results of quantum chemical calculations, in particular for

Table 5. Logarithms of the formation constants (logβ) for mixed-ligand zinc(II) complexes with L/D-amino acids (HisH, CysH, MetH, SerH, TrpH, PheH) (25.0 °C, 1.0 *M* KNO_3)

Equilibrium	Amino acid residues	logβ	Δlogβ
$Zn^{2+} + His^- + Cys^{2-} \rightleftharpoons [Zn(His)(Cys)]^-$	L-Cys, L-His	15.17(1)	
	L-Cys, D-His	15.26(1)	*−0.09*
$Zn^{2+} + His^- + Cys^{2-} \rightleftharpoons [Zn(His)(Cys)(OH)]^{2-} + H^+$	L-Cys, L-His	4.43(2)	
	L-Cys, D-His	4.55(2)	*−0.12*
$Zn^{2+} + His^- + Met^- \rightleftharpoons Zn(His)(Met)$	L-Met, L-His	10.427(5)	
	L-Met, D-His	10.435(4)	−0.008
$Zn^{2+} + His^- + Ser^- \rightleftharpoons Zn(His)(Ser)$	L-Ser, L-His	10.38(1)	
	D-Ser, L-His	10.372(8)	0.01
$Zn^{2+} + His^- + Thr^- \rightleftharpoons Zn(His)(Thr)$	L-Thr, L-His	10.822(5)	
	L-Thr, D-His	10.824(5)	−0.002
$Zn^{2+} + His^- + Phe^- \rightleftharpoons Zn(His)(Phe)$	L-Phe, L-His	10.500(4)	
	D-Phe, L-His	10.555(5)	*−0.055*
$Zn^{2+} + His^- + Trp^- \rightleftharpoons Zn(His)(Trp)$	L-Trp, L-His	10.776(8)	
	D-Trp, L-His	10.897(7)	*−0.121*

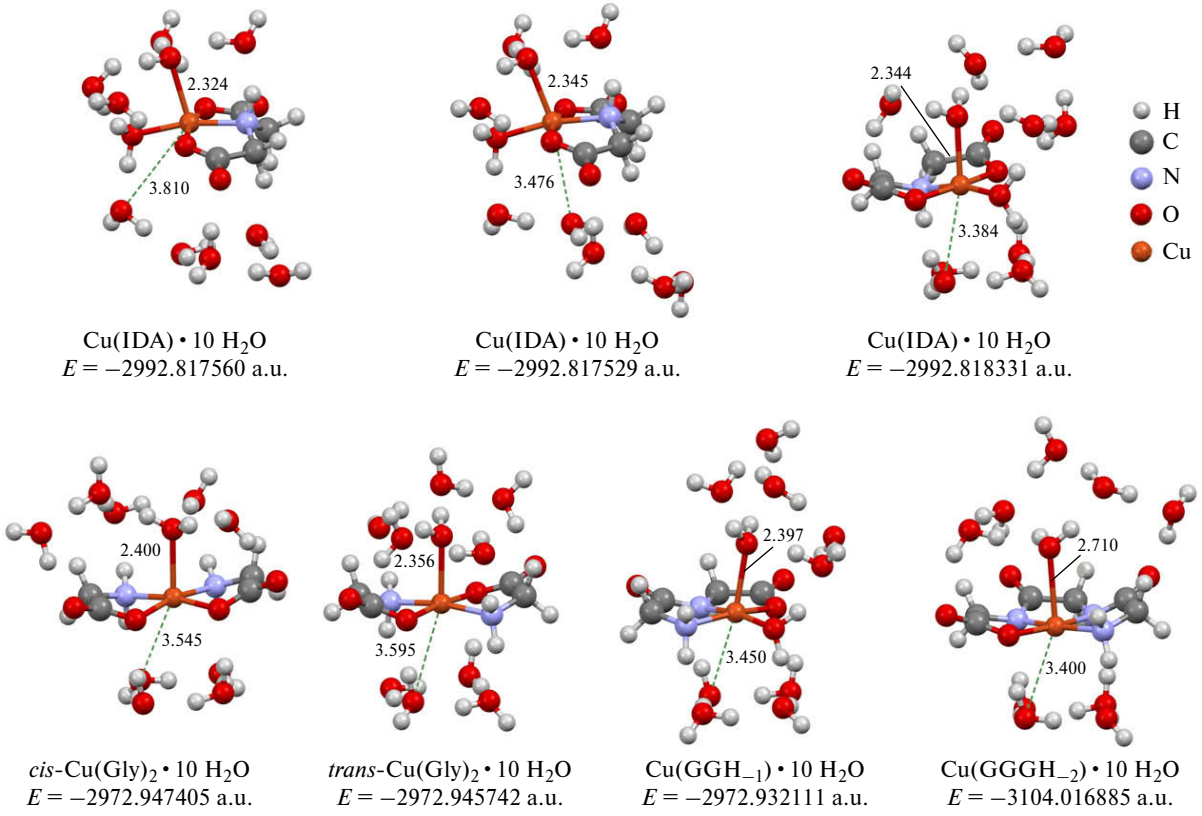

Fig. 3. Structures and total energies of copper(II) complexes with N,O-containing ligands optimized at the CAM-B3LYP/TZVP level of theory taking into account the solvent effects by the C-PCM model (distances are given in Å).[15]

copper(II) complexes with iminodiacetic acid ($IDAH_2$), glycine (GlyH), di- and triglycines (GGH and GGGH) in the environment of 10 water molecules (Fig. 3). As can be seen in Fig. 3, only one axial water molecule is present in all these complexes, and the rings of four hydrogen-bonded water molecules are located on the opposite side at significant distances.[15]

The five-coordinate state of copper(II) is confirmed by the results of MD calculations, which were performed using the GROMACS package[17] with a slightly modified FFWa-SPCE force field [18] and the GROMOS force field.[19] The results of these calculations for aqueous solutions demonstrated that the average number of water molecules in the first coordination sphere of copper(II) bis-complexes is always smaller than two.[16] Note that the radial distribution functions of oxygen atoms in the second coordination sphere of the *trans* isomers with glycine, serine, lysine ($LysH_2^+$), and aspartic acid have one maximum, whereas there are two maxima for the *cis* isomers (Fig. 4). The presence of two maxima is due to the fact that the field of adjacent *cis*-carboxy groups more strongly attracts the nearest water molecules, particularly in the complex *cis*-$[Cu(Asp)_2]^{2-}$.

It is worth noting that the five-coordinate state of copper(II) in the complex $CuCl_2L^1L^2H_2O$ (L^1 = 2-amino-4-methylpyrimidine, L^2 = 2,3-diaminopyridine) was recently confirmed by the quantum chemical calculations at the DFT/B3LYP level.[20] This casts doubt on the explanation of the difference in the stability constants of the copper(II) complexes with *N*-[tris(hydroxymethyl)methyl]-β-alanine and with *N*-[2-hydroxy-1,1-bis(hydroxymethyl)ethyl]-β-alanine (tricine) given in the study[21] on the assumption of the octahedral coordination of these complexes with reference to the study.[22] In the cited study, a weak axial coordination of two alcoholic groups in the tetragonally distorted octahedron was found in the crystal of the bis[*N*-(2-hydroxyethyl)-β-alaninato]copper(II) complex. This octahedral coordination of copper(II) in solution is unlikely.

The use of a combination of different methods (DFT, MD, and NMR relaxation) allows one to obtain complete information on the structure and the dynamic behavior of the first and second hydr-

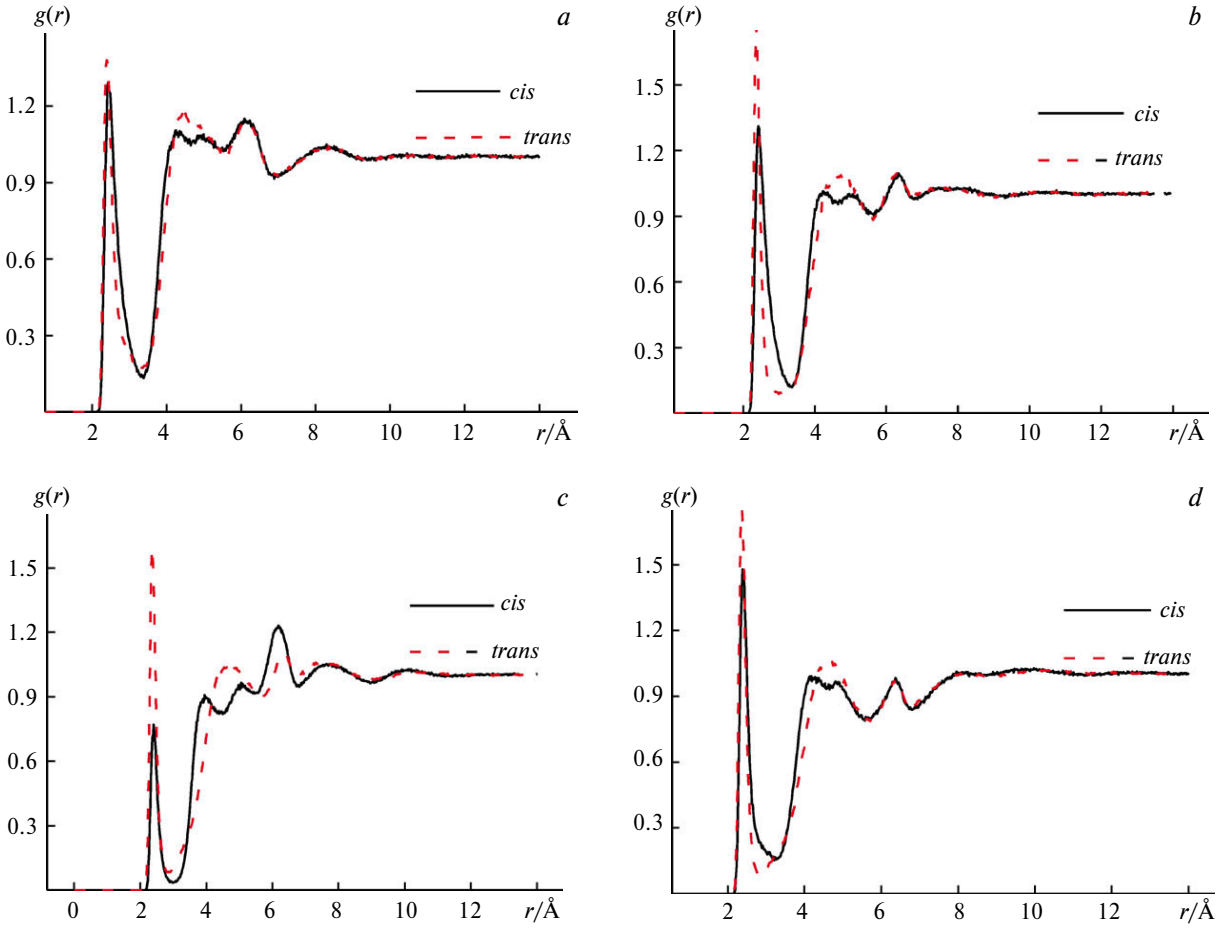

Fig. 4. Radial distribution functions (RDF) for Cu^{II}—O(H_2O) solvated complexes calculated from the results of MD simulations for 10 ns at 25 °C: $Cu(Glu)_2$ (*a*), $Cu(Ser)_2$ (*b*), $[Cu(Asp)_2]^{2-}$ (*c*), and $[Cu(LysH)_2]^{2+}$ (*d*).[16]

ation shells of copper(II) complexes in good agreement with the experimental data (Table 6).[16,23] It should be noted that the level of theory in the calculations has a significant effect on the accuracy of the results. As can be seen in Table 7, only calculations at the CAM-B3LYP/TZVP level taking into account 10 water molecules in the solvation shell and using the polarizable continuum solvent model C-PCM provide the results, which are in agreement with the X-ray diffraction data for the crystals of all the copper(II) complexes under consideration (given in italic).[16] Nevertheless, investigations of crystal solvates (hydrates and peroxosolvates) with biomolecules, in particular with amino acids, will be of ever greater value for a deeper understanding of the important role of hydrogen bonding in solutions of metal complexes with bioligands and their analogs. The available data in this area were reported in the studies[24,25] (see also references therein).

The d—π interaction, which is manifested in the effect of the ligand nature on the spin-Hamiltonian parameters determined from the EPR spectra of the copper(II) complexes with di- and tripeptides (Table 8), is an important factor responsible for the stereoselectivity.[26—28] Thus, the introduction of an aromatic substituent, phenyl (Phe) or phenoxy (Tyr ≡ Y), into di- or triglycine leads to a decrease in the *g*-factor and an increase in the isotropic hfc constant (A_0), which is indicative of the axial binding of electron-withdrawing groups, being an evidence of a d—π interaction. The blocking of the only axial position by an aromatic substituent of oligopeptide hinders the coordination of other ligands. For this reason, the significant stereoselectivity is manifested in the formation of mixed-ligand complexes containing glycyl-L-tyrosine (GYH) and L- or D-histidine, including the binuclear complex $Cu_2(GY\cdot H_{-1})(His)_2$, unlike related complexes with diglycine, in which the stereoselectivity is absent (Table 9).

Table 6. Results of DFT calculations of the radial distribution functions (RDF) for Cu^{II}—$O(H_2O)$ and Cu^{II}—$H(H_2O)$ and the experimental NMR relaxation data: r_1, r_{Hi}, and CN_i are the distance between Cu^{II} and the water oxygen atom, the distance between Cu^{II} and the water hydrogen atoms, and the average number of molecules in the *i*-th coordination sphere, respectively, τ_{M2} is the average lifetime for the second coordination sphere of water molecules[16]

Complex	DFT		MD calculation					NMR relaxation			
	r_1	r_1	CN_1	r_2/Å	CN_2	r_{H_1}	r_{H_2}	r_{H_1}	r_{H_2}	τ_{M2}/ps	
	Å					Å		Å		theor.	exp.
$Cu(Gly)_2$											
cis isomer	2.40	2.44	1.8	4.3	7.7	3.08	4.8	3.1	4.0	5.5	5(1)
trans isomer	2.36	2.40	1.6	4.4	7.6	3.15	—[a]	—[b]	—[b]	4.9	—[b]
$Cu(L\text{-}Ser)_2$											
cis isomer	2.47	2.43	1.7	4.3	6.8	3.10	4.8	3.2	4.05	6.3	10(2)
trans isomer	2.43	2.37	1.1	4.6	7.1	3.07	—[a]	—[b]	—[b]	5.7	—[b]
$[Cu(L\text{-}Asp)_2]^{2-}$											
cis isomer	2.38	2.41	*0.5*	*4.0*	*6.0*	3.10	4.8	3.2	4.15	*15.4*	11(2)
trans isomer	2.35	2.37	0.9	4.7	~8	2.83, 3.22	4.8	—[b]	—[b]	9.7	—[b]
$[Cu(L\text{-}LysH)_2]^{2+}$											
cis isomer	2.36	2.40	1.4	4.2	7.4	3.10	4.7	3.2	4.05	7.4	9(2)
trans isomer	2.34	2.38	1.0	4.6	~8	3.13	—[a]	—[b]	—[b]	7.0	—[b]

[a] Second and third coordination sphere water molecules are indistinguishable in the RDF for Cu^{II}—H_{water}.
[b] The *cis* and *trans* isomers are indistinguishable by the NMR relaxation method.

Table 7. The Cu^{II}—O (r_O/Å) and Cu^{II}—H (r_{H1}/Å, r_{H2}/Å) distances for the axial water molecule in the structures optimized at the B3LYP/aug-cc-pVTZ, B3LYP/TZVP, and CAM-B3LYP/TZVP levels of theory taking into account the C-PCM solvent model for different numbers of water molecules in the solvent shell[15]

Complex	B3LYP/aug-cc-pVTZ with C-PCM and 1 H_2O molecule			B3LYP/TZVP with C-PCM and 1 H_2O molecule			CAM-B3LYP/TZVP with C-PCM and 1 H_2O molecule			CAM-B3LYP/TZVP with C-PCM and 10 H_2O molecules			XRD data (see Ref. 15 and references therein) r_O
	r_O	r_{H_1}	r_{H_2}	r_O	r_{H_1}	r_{H_2}	r_O	r_{H_1}	r_{H_2}	r_O	r_{H_1}	r_{H_2}	
Cu(IDA)	2.46	3.04	3.08	2.37	2.98	3.01	2.31	2.92	2.95	*2.34*	2.88	2.97	*2.38*
trans-$Cu(Gly)_2$	2.49	3.05	3.17	2.43	2.99	3.10	2.36	2.92	3.05	*2.36*	2.91	2.93	—
cis-$Cu(Gly)_2$	2.56	2.83	3.21	2.48	2.89	3.10	2.40	2.83	3.14	*2.40*	2.91	2.99	*2.40*
$Cu(GGH_{-1})$	2.54	3.06	3.06	2.47	3.00	3.01	2.39	2.94	2.95	*2.40*	2.98	3.09	*2.3—2.39*
$[Cu(GGGH_{-2})]^-$	4.17	4.34	4.94	4.17	4.35	4.96	4.13	4.32	4.92	*2.71*	3.03	3.40	*2.57*

Table 8. Parameters of EPR spectra of copper(II) complexes with di- and tripeptides (LH) (25 °C, 1.0 *M* KNO_3); τ_R is the rotational correlation time

System	Complex	g_0	A_0	A_N	$\tau_R \cdot 10^{11}$/s
			G		
Cu^{II}—GlyGlyH	$CuLH_{-1}$	2.1232(2)	67.7(2)	14.2(3), 11.8(4)	3.4(2)
	$[Cu(LH_{-1})(OH)]^-$	2.1190(2)	37.2(3)	12.5(2), 12.2(2)	5.3(2)
Cu^{II}—GlyTyrH	$CuLH_{-1}$	*2.1207(2)*	*71.4(2)*	14.1(2), 11.7(3)	6.3(2)
	$[Cu(LH_{-1})(OH)]^-$	2.1164(2)	42.0(3)	12.6(2), 12.2(2)	10.7(6)
Cu^{II}—TyrLeuH	$CuLH_{-1}$	*2.1196(2)*	*72.0(3)*	14.3(3), 11.8(4)	7.0(4)
	$[Cu(LH_{-1})(OH)]^-$	2.1137(3)	43.3(4)	12.5(3), 12.0(3)	12.9(8)
Cu^{II}—TyrPheH	$CuLH_{-1}$	*2.1202(2)*	*71.7(2)*	14.3(3), 11.7(4)	8.5(6)
	$[Cu(LH_{-1})(OH)]^-$	2.1161(3)	42.4(4)	12.6(2), 12.5(2)	12.8(7)
Cu^{II}—TyrTyrH	$CuLH_{-1}$	*2.1187(2)*	*69.6(2)*	14.5(2), 11.4(2)	10.3(5)
	$[Cu(LH_{-1})(OH)]^-$	2.1163(2)	42.4(2)	12.5(1), 12.4(1)	19(1)
Cu^{II}—GlyGlyGlyH	$[Cu((LH_{-2})]^-$	2.0947(3)	80.9(2)	17.2(3), 14.5(3), 8.4(3)	4.3(1)
Cu^{II}—GlyGlyTyrH	$[Cu(LH_{-2})]^-$	*2.0918(2)*	*83.6(2)*	17.5(2), 14.6(2), 8.2(3)	8.0(2)
	$[Cu(LH_{-3})]^{2-}$	*2.0925(2)*	*83.0(2)*	17.2(2), 14.7(2), 8.3(3)	9.5(3)

Table 9. Logarithms of the formation constants (logβ) for mixed-ligand complexes in copper(II)—L/D-HisH—dipeptide (glycylglycine (GlyGlyH≡GGH)/glycyl-L-tyrosine (GlyTyrH ≡ GYH)) systems (25.0 °C, 1.0 *M* KNO_3)

Equilibrium	logβ		Δlogβ
	L-His	D-His	
$Cu^{2+} + GG^- + HisH \rightleftharpoons [Cu(GG)(HisH)]^+$	10.74(2)	10.75(2)	−0.010
$Cu^{2+} + GG^- + His^- \rightleftharpoons Cu(GG)(His)$	15.416(7)	15.410(7)	0.006
$Cu^{2+} + GG^- + His^- \rightleftharpoons [Cu(GG \cdot H_{-1})(His)]^- + H^+$	6.91(1)	6.88(3)	0.030
$Cu^{2+} + GG^- + His^- \rightleftharpoons [Cu(GG \cdot H_{-1})(HisH_{-1})]^{2-} + 2\ H^+$	−4.49(1)	−4.46(2)	−0.030
$2\ Cu^{2+} + GG^- + 2\ His^- \rightleftharpoons Cu_2(GG \cdot H_{-1})(His)_2 + H^+$	21.90(4)	21.87(5)	0.030
$Cu^{2+} + GY^- + HisH \rightleftharpoons [Cu(GY)(HisH)]^+$	10.64(3)	10.65(3)	−0.010
$Cu^{2+} + GY^- + His^- \rightleftharpoons Cu(GY)(His)$	15.455(9)	15.421(9)	0.034
$Cu^{2+} + GY^- + His^- \rightleftharpoons [Cu(GY \cdot H_{-1})(His)]^- + H^+$	7.00(1)	6.87(1)	*0.13*
$Cu^{2+} + GY \cdot H_{-1}^{2-} + His^- \rightleftharpoons [Cu(GY \cdot H_{-2})(His)]^{2-} + H^+$	6.857(7)	6.817(7)	*0.040*
$2\ Cu^{2+} + GY^- + 2\ His^- \rightleftharpoons Cu_2(GY \cdot H_{-1})(His)_2 + H^+$	22.89(1)	22.75(1)	*0.14*

According to the quantum chemical calculations (Fig. 5), the stereoselectivity of the formation of two mixed-ligand complexes with glycyl-L-tyrosine is attributed to the fact that the amino group of histidine is in the *cis* position due to the strong *trans* effect of the deprotonated peptide nitrogen atom. The isomers with four equatorially coordinated nitrogen atoms are the most favorable in the case of L-histidine; in the case of D-histidine, one carboxy group is present in the equatorial plane. Note that the stereoselectiv-

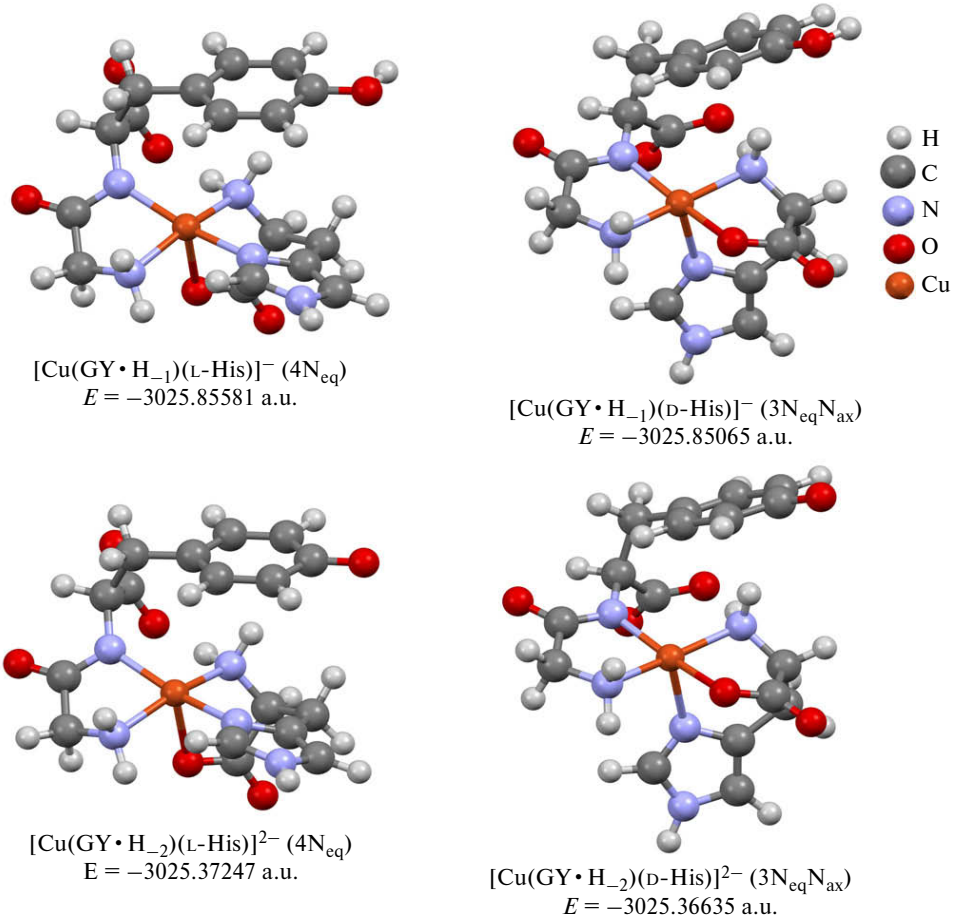

Fig. 5. Structures and total energies of mixed-ligand copper(II) complexes with glycyl-L-tyrosine (GYH) and L/D-histidine (HisH) optimized using the ORCA package at the CAM-B3LYP/TZVP level of theory taking into account the solvent effects by the C-PCM model.

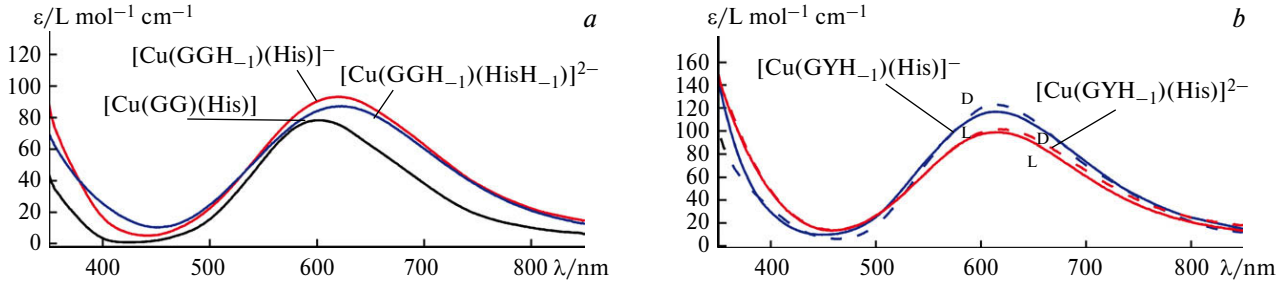

Fig. 6. Simulated absorption spectra of mixed-ligand copper(II) complexes with L/D-histidine (HisH) and glycylglycine (GGH) (*a*) and with glycyl-L-tyrosine (GYH) (*b*); 25 °C, 1.0 *M* KNO_3.

ity is manifested also in the absorption spectra of the corresponding complexes (Fig. 6).

Five and six mixed-ligand complex forms (Table 10), including binuclear structures, are produced in ternary systems with histidine, triglycine (GGGH), and glycylglycyl-L-tyrosine (GGYH), respectively. The stereoselectivity of the formation is observed only for the complex Cu(GGY)(His). According to the results of calculations, the most favorable structure of the complex with the L isomer of amino acid (Fig. 7) is that in which the amino groups of adjacent ligands are *cis* to each other, thereby providing a π—π-stacking interaction between the phenoxy and imidazole groups, which is impossible for the *trans* isomers.

The modified fast-motion program[29] and the EasySpin program package[30] in the slow-motion mode in combination with the STALABS-M program allow the simulation of the EPR spectra and the electronic absorption spectra of many resulting forms of the complexes (Fig. 8), thus revealing the stereoselectivity of the formation of one of these complexes, Cu(GGY)(His).[28]

The kinetics of substitution reactions of oligopeptide ligands with histidine under pseudo-first-order conditions was studied by the stopped-flow method.[27,28] The plots presented in Fig. 9 show that an increase in pH leads to an increase in the rate of substitution. The scheme consisting of three and two steps was proposed for the replacement of tri- and dipeptide ligands, respectively, with histidine (Scheme 1).

In both cases, the last step is rate-determining, both the anionic and protonated forms of histidine being active in the substitution (with the constants k_3 and k_3', respectively). As can be seen in Table 11, the presence of a phenoxy group leads to a decrease in the rate of the ligand substitution for both dipeptides and tripeptides, which is due to the fact that one axial position of copper(II), as the site of attack by the ligand, is sterically blocked by the tyrosine side group. The statistically significant stereoselectivity is observed for the replacement of glycyl-L-tyrosine or glycylglycyl-L-tyrosine with the histidinate anion (see Table 11).

Table 10. Logarithms of the formation constants (logβ) for mixed-ligand complexes in copper(II)—L/D-HisH—tripeptide (glycylglycylglycine (GGGH)/glycylglycyl-L-tyrosine (GGYH)) systems (25.0 °C, 1.0 *M* KNO_3)[27,28]

Equilibrium	logβ		Δlogβ
	L-His	D-His	
$Cu^{2+} + GGG^- + HisH \rightleftharpoons [Cu(GGG)(HisH)]^+$	10.56(2)	10.58(2)	−0.02
$Cu^{2+} + GGG^- + His^- \rightleftharpoons Cu(GGG)(His)$	14.915(5)	14.906(6)	0.011
$Cu^{2+} + GGG^- + His^- \rightleftharpoons [Cu(GGG\cdot H_{-1})(His)]^- + H^+$	6.39(2)	6.36(2)	0.03
$Cu^{2+} + GGG^- + His^- \rightleftharpoons [Cu(GGG\cdot H_{-2})(His)]^{2-} + 2\,H^+$	−4.141(8)	−4.126(9)	0.015
$2\,Cu^{2+} + GGG^- + 2\,His^- \rightleftharpoons [Cu_2(GGG\cdot H_{-2})(His)(HisH_{-1})]^{2-} + 3\,H^+$	1.99(8)	2.04(8)	−0.05
$Cu^{2+} + GGY^- + HisH \rightleftharpoons [Cu(GGY)(HisH)]^+$	10.75(1)	10.76(1)	−0.01
$Cu^{2+} + GGY^- + His^- \rightleftharpoons Cu(GGY)(His)$	15.086(3)	14.983(4)	*0.103*
$Cu^{2+} + GGY^- + His^- \rightleftharpoons [Cu(GGY\cdot H_{-1})(His)]^- + H^+$	6.72(1)	6.74(2)	−0.02
$Cu^{2+} + [GGY\cdot H_{-1}]^{2-} + His^- \rightleftharpoons [Cu(GGY\cdot H_{-2})(His)]^{2-} + H^+$	6.94(1)	6.91(2)	0.03
$2\,Cu^{2+} + GGY^- + 2\,His^- \rightleftharpoons Cu_2(GGY\cdot H_{-1})(His)_2 + H^+$	20.65(9)	20.61(8)	0.04
$2\,Cu^{2+} + [GGY\cdot H_{-1}]^{2-} + 2\,His^- \rightleftharpoons [Cu_2(GGY\cdot H_{-3})(His)(HisH_{-1})]^{3-} + 3\,H^+$	2.34(5)	2.37(6)	−0.03

Scheme 1

$$v = k_{obs}[[Cu(LH_{-2})]^-] = (k_0 + k_L[His^-] + k_{LH}[HisH])[[Cu(LH_{-2})]^-]$$

$$k_{obs} = k_0 + k_L[His^-] + k_{LH}[HisH] = k_0 + k_{LH} \cdot C_{HisH} + (k_L - k_{LH})[His^-]$$

$$Cu(LH_{-2})^- + His^- \underset{k_{-1}}{\overset{k_1}{\rightleftharpoons}} [Cu(LH_{-2})(His)]^{2-}$$

$$[Cu(LH_{-2})(His)]^{2-} + H_2O \underset{k_{-2}}{\overset{k_2}{\rightleftharpoons}} [Cu(LH_{-1})(His)]^- + OH^-$$

$$[Cu(LH_{-1})(His)]^- + His^- + H_2O \xrightarrow{k_3} Cu(His)_2 + L^- + OH^-$$

$$[Cu(LH_{-1})(His)]^- + HisH \xrightarrow{k_3'} Cu(His)_2 + L^-$$

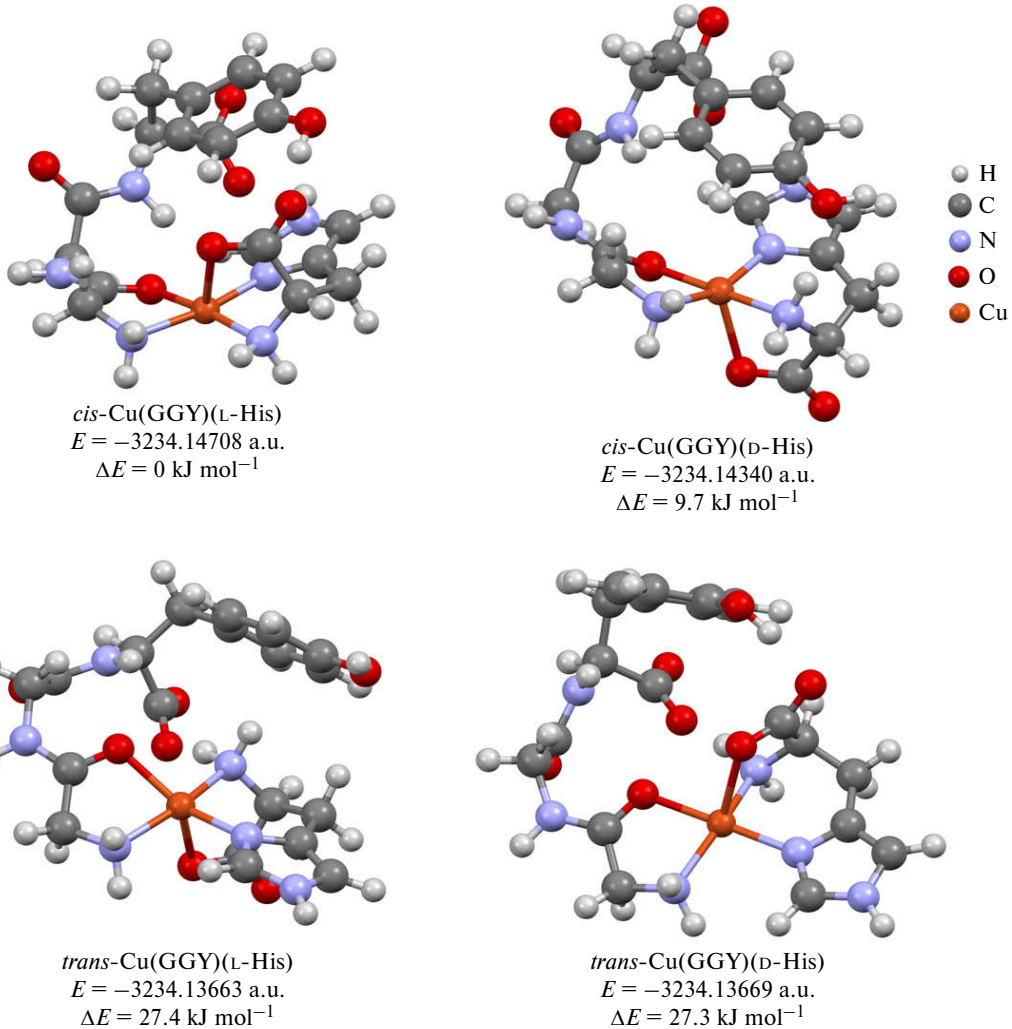

cis-Cu(GGY)(L-His)
$E = -3234.14708$ a.u.
$\Delta E = 0$ kJ mol^{-1}

cis-Cu(GGY)(D-His)
$E = -3234.14340$ a.u.
$\Delta E = 9.7$ kJ mol^{-1}

trans-Cu(GGY)(L-His)
$E = -3234.13663$ a.u.
$\Delta E = 27.4$ kJ mol^{-1}

trans-Cu(GGY)(D-His)
$E = -3234.13669$ a.u.
$\Delta E = 27.3$ kJ mol^{-1}

Fig. 7. Structures and total energies of the most stable mixed-ligand copper(II) complexes with glycylglycyl-L-tyrosine (GGYH) and L/D-histidine (HisH) optimized at the CAM-B3LYP/TZVP level of theory including the solvent effects by the C-PCM model and with the D3BJ dispersion correction.[28]

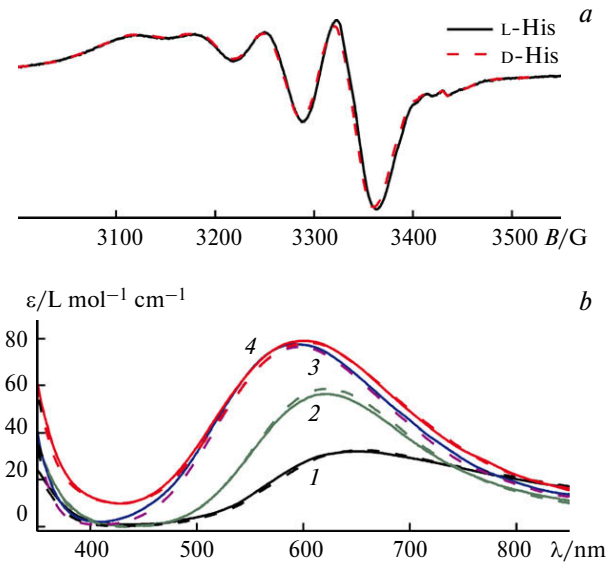

Fig. 8. Experimental EPR spectra for the copper(II)—glycylglycyl-L-tyrosine—L/D-histidine systems (1 : 1 : 1) (pH 6.60, 25 °C) (*a*) and the simulated absorption spectra of the mixed-ligand copper(II) complexes with glycylglycyl-L-tyrosine (GGYH) and L/D-histidine (HisH) at 25 °C (*b*), 1.0 *M* KNO_3: *1*, $[Cu(GGY)(HisH)]^+$; *2*, Cu(GGY)(His); *3*, $[Cu(GGY\cdot H_{-1})(His)]^-$; *4*, $[Cu(GGY\cdot H_{-2})(His)]^{2-}$.[27,28]

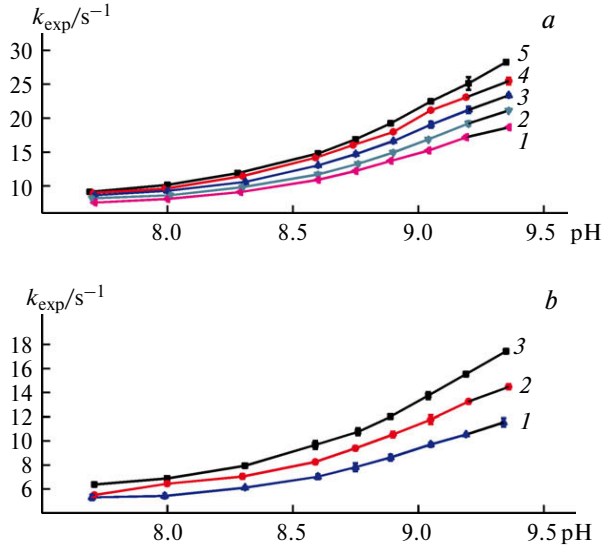

Fig. 9. Plots of the observed rate constants (k_{exp}) *versus* pH in the copper(II)—glycylglycylglycine—L-histidine systems (1 : 1 : 10) (*a*; His concentration: 0.03 (*1*), 0.032 (*2*), 0.040 (*3*), 0.045 (*4*), 0.05 mol L^{-1} (*5*)) and the copper(II)—glycylglycyl-L-tyrosine—L-histidine systems (1 : 1 : 10) (*b*; His concentration: 0.03 (*1*), 0.04 (*2*), 0.05 mol L^{-1} (*3*)) obtained by the stopped-flow method by mixing equivalent volumes of solutions I and II with the detection at λ = 550 nm (*l* = 1 cm); I, Cu^{II}, GGH·H (*a*)/Cu^{II}, GGY·H (*b*); II, L-HisH (*a*, *b*); C_{Tris} = 0.1 mol L^{-1}, *T* = 298 K.[27,28]

Copper(II) complexes with phosphorylated dithiocarbamates (PDTC), which were synthesized for the first time in the study,[31] are of particular interest. As can be seen in Table 12, the formation constants of mixed-ligand complexes with these dithiocarbamates and aromatic N-donors, including 1,10-phenanthroline (phen) and 2-methylpyrido[3,2-*f*:2′,3′-*h*]-quinoxaline (MeDPQ), which were determined by SP-metry, provide evidence of significant extra-stabilization of these complexes according to the standard criterion $\log X = 2\log\beta_{MAB} - \log\beta_{MA_2} - \log\beta_{MB_2}$ (the indices correspond to the mixed-ligand complex of the composition MAB and homo-ligand bis-complexes of the compositions MA_2 and MB_2, respectively; the statistical evaluation $\log X = 0.60$). This fact is attributed to the strong d—π interaction with the electron density transfer as from the π-donor orbitals of carboxy groups of amino acids through the central ion to the π-acceptor orbitals of aromatic N-donors. It is important that these complexes exhibit the highest antineoplastic activity among all the compounds characterized in our studies.[32]

Table 11. Rate constants of the substitution reactions of oligopeptide ligands from copper(II) complexes with L/D/DL-histidine (25 °C, 1.0 *M* KNO_3, Tris buffer)[27,28]

Complex	Amino acid	k_0/s^{-1}	k_{LH}	k_L
			mol^{-1} L s^{-1}	
$Cu(GG\cdot H_{-1})$	L-Histidine	0.7±0.1	34.9±1.6	359±6
$Cu(GG\cdot H_{-1})$	DL-Histidine	0.9±0.1	32.8±2.0	337±7
$Cu(GY\cdot H_{-1})$	L-Histidine	0.20±0.01	—	*26.7±1.0*
$Cu(GY\cdot H_{-1})$	D-Histidine	0.25±0.01	—	*21.8±0.7*
$[Cu(GGG\cdot H_{-2})]^-$	L-Histidine	4.9±0.2	68.7±6.0	*740±6*
$[Cu(GGG\cdot H_{-2})]^-$	DL-Histidine	4.1±0.3	87.7±8.5	*782±6*
$[Cu(GGY\cdot H_{-2})]^-$	L-Histidine	3.46±0.03	44.9±0.7	*439±5*
$[Cu(GGY\cdot H_{-2})]^-$	D-Histidine	3.37±0.10	43.9±3.1	*459±3*

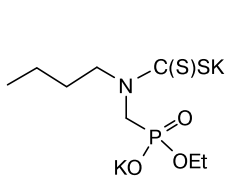

$K_2Bu(OEt)PDTC$

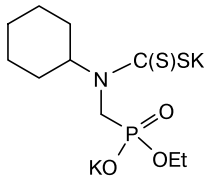

$K_2cHex(OEt)PDTC$

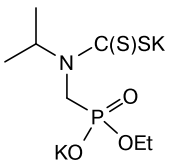

$K_2Pr^i(OEt)PDTC$

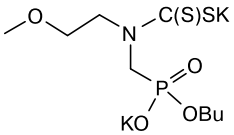

$K_2EtOMe(OBu)PDTC$

Table 12. Formation constants of copper(II) complexes with phosphorylated dithiocarbamates and aromatic N-donors, phen and MeDPQ (37.0 °C, 0.15 *M* NaCl)

Ligand (PDTS)	$[Cu(PDTC)_2]^{2-}$ logβ	Cu(phen)(PDTC)		Cu(MeDPQ)(PDTC)	
		logβ	log*X*	logβ	log*X*
$[Bu(OEt)PDTC]^{2-}$	16.3(2)	16.96(6)	3.32	16.64(5)	*4.49*
$[cHex(OEt)PDTC]^{2-}$	16.8(4)	17.17(3)	3.21	17.01(3)	*4.71*
$[Pr^i(OEt)PDTC]^{2-}$	16.30(2)	16.83(5)	3.06	16.50(4)	*4.21*
$[EtOMe(OBu)PDTC]^{2-}$	16.7(1)	16.17(3)	2.71	16.34(6)	*3.54*

It is worth noting that new isonicotinoyl hydrazones with vitamin B_6 derivatives were synthesized in the Scientific and Educational Center of Pharmaceutics of the Kazan Federal University. One of these compounds, (*E*/*Z*)-*N*′-{[5-hydroxy-3,4-bis(hydroxymethyl)-6-methylpyridin-2-yl]methylene}isonicotinohydrazide (LH), exhibited high antibacterial activity.[33] The structure of the new ligand LH as the *E* isomer (Fig. 10) was determined by X-ray diffraction,[33] and the formation constants of a series of 3d metal complexes with this ligand were determined by SP-metry. The lead ligand (LH) is a promising candidate as an antituberculosis agent, the activity of which is much higher than that of the known agent pyridoxal isonicotinoyl hydrazone (PIH).[33]

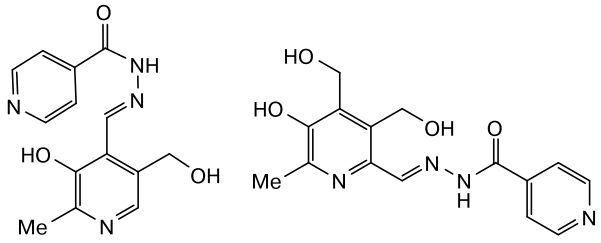

Research in this area is being continued.

Therefore, the main factors controlling the stereoselectivity of the complexation, the stability of the complexes, and the kinetics of ligand substitution reactions are as follows:

— *trans* effect;

— solvation interactions;

— intracomplex hydrogen bonding;

— new type of a weak thiomethyl group—imidazole ring interaction;

— softness of ligands and the central ion;

— π—π-stacking interactions;

— effect of interligand hydrogen bonds;

— the five-coordinate environment of copper(II) in solution;

— metal—ligand d—π interaction;

— steric blocking of the axial position of copper(II).

Note that the methodology of investigations, which allows one to obtain complete data on coordination compounds, requires the competent use of a number of complementary spectroscopic methods, including SP-metry, EPR, and NMR relaxation, X-ray diffraction analysis, the stopped-flow spectrophotometric method, and pH-metry, combined with mathematical modeling methods using modern programs and accurate calculations by MD and high-level quantum chemical methods.

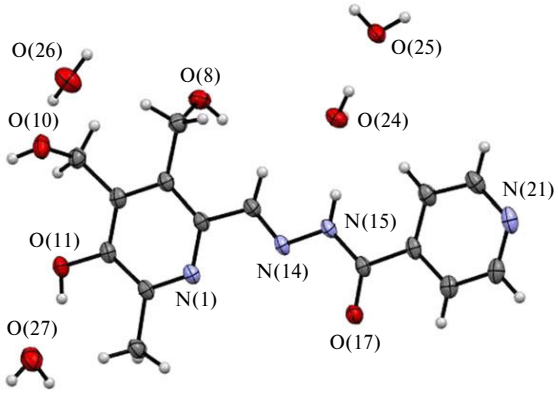

Fig. 10. X-ray diffraction structure of the *E* isomer of LH.[33]

The study was financially supported by the Government Program for Enhancing Competitive Ranking of Kazan Federal University, the Subsidy allocated to Kazan Federal University for the state assignment in the sphere of scientific activities by the Ministry of Science and Higher Education of the Russian Federation (Program No. 0671-2020-0061), and the Russian Science Foundation (Project Nos 16-33-00674, 16-33-00691, 18-33-20072, and 20-33-90235).

No human or animal subjects were used in this research.

The authors declare no competing interests.

References

1. V. G. Shtyrlin, N. Yu. Serov, M. S. Bukharov, E. M. Gilyazetdinov, M. A. Zhernakov, M. A. Ahmed, A. R.

Garifzyanov, I. I. Mirzayanov, A. V. Ermolaev, N. S. Aksenin, K. V. Urazaeva, A. V. Zakharov, *Spektroskopiya koordinatsionnykh soedinenii* (*Sb. nauch. trudov XIX Mezhd. konf.*) [*Spectroscopy of Coordination Compounds (Coll. of Sci. Reports of the XIX Int. Conf.)*] *(Tuapse, September 18—23, 2022)*, Krasnodar, Kubanskii Gos. Un-t, 2022, p. 210 (in Russian).

2. A. A. Krutikov, V. G. Shtyrlin, A. O. Spiridonov, N. Yu. Serov, A. N. Il´yin, M. S. Bukharov, E. M. Gilyazetdinov, *J. Phys. Conf. Ser.*, 2012, **394**, 012031; DOI: 10.1088/1742-6596/394/1/012031.
3. V. G. Shtyrlin, E. M. Gilyazetdinov, N. Yu. Serov, D. F. Pyreu, M. S. Bukharov, A. A. Krutikov, N. S. Aksenin, A. I. Gizatullin, A. V. Zakharov, *Inorg. Chim. Acta*, 2018, **477**, 135—147; DOI: 10.1016/j.ica.2018.02.018.
4. M. W. Schmidt, K. K. Baldridge, J. A. Boatz, S. T. Elbert, M. S. Gordon, J. H. Jensen, S. Koseki, N. Matsunaga, K. A. Nguyen, S. J. Su, T. L. Windus, M. Dupuis, J. A. Montgomery, *J. Comput. Chem.*, 1993, **14**, 1347—1363; DOI: 10.1002/jcc.540141112.
5. F. Neese, *WIREs Comput. Molec. Sci.*, 2012, **2**, 73—78; DOI: 10.1002/wcms.81.
6. W. Kohn, A. D. Becke, R. G. Parr, *J. Phys. Chem.*, 1996, **100**, 12974—12980; DOI: 10.1021/jp960669l.
7. A. D. Becke, *J. Chem. Phys.*, 1993, **98**, 5648—5652; DOI: 10.1063/1.464913.
8. C. Lee, W. Yang, R. G. Parr, *Phys. Rev. B*, 1988, **37**, 785—789; DOI: 10.1103/PhysRevB.37.785.
9. T. Yanai, D. P. Tew, N. C. Handy, *Chem. Phys. Lett.*, 2004, **393**, 51—57; DOI: 10.1016/j.cplett.2004.06.011.
10. A. Schäfer, C. Huber, R. Ahlrichs, *J. Chem. Phys.*, 1994, **100**, 5829—5835; DOI: 10.1063/1.467146.
11. J. P. Perdew, K. Burke, M. Ernzerhof, *Phys. Rev. Lett.*, 1996, **77**, 3865—3868; DOI: 10.1103/PhysRevLett.77.3865.
12. M. Cossi, N. Rega, G. Scalmani, V. Barone, *J. Comput. Chem.*, 2003, **24**, 669—681; DOI: 10.1002/jcc.10189.
13. E. M. Gilyazetdinov, V. G. Shtyrlin, N. Yu. Serov, L. A. Romanova, M. S. Bukharov, *Tez. dokl. XX Mendeleevskogo s´ezda po obshchei i prikladnoi khimii* [*Abstr. of Papers of XX Mendeleev Congress on General and Applied Chemistry*] *(Yekaterinburg, September 26—30, 2016*), Uralskoe otdelenie RAN, 2016, **1**, p. 168 (in Russian).
14. E. M. Gilyazetdinov, M. S. Bukharov, L. A. Romanova, N. Yu. Serov, V. G. Shtyrlin, *27th Int. Chugaev Conf. on Coordination Chemistry (Nizhny Novgorod, October 2—6, 2017)*, *Book of Abstracts*, Nizhny Novgorod, 2017, p. 32.
15. M. S. Bukharov, V. G. Shtyrlin, G. V. Mamin, S. Stapf, C. Mattea, A. S. Mukhtarov, N. Yu. Serov, E. M. Gilyazetdinov, *Inorg. Chem.*, 2015, **54**, 9777—9784; DOI: 10.1021/acs.inorgchem.5b01467.
16. M. S. Bukharov, V. G. Shtyrlin, E. M. Gilyazetdinov, N. Yu. Serov, T. I. Madzhidov, *J. Comput. Chem.*, 2018, **39**, 821—826; DOI: 10.1002/jcc.25154.
17. M. J. Abraham, T. Murtola, R. Schulz, S. Pall, J. C. Smith, B. Hess, E. Lindahl, *SoftwareX*, 2015, **1—2**, 19; DOI: 10.1016/j.softx.2015.06.001.
18. J. Sabolović, V. Gomzi, *J. Chem. Theory Comput.*, 2009, **5**, 1940—1954; DOI: 10.1021/ct9000203.
19. N. Schmid, A. P. Eichenberger, A. Choutko, S. Riniker, M. Winger, A. E. Mark, W. F. van Gunsteren, *Eur. Biophys. J.*, 2011, **40**, 843—856; DOI: 10.1007/s00249-011-0700-9.
20. M. S. Al-Fakeh, S. Messaoudi, F. I. Alresheedi, A. E. Albadri, W. A. El-Sayed, E. E. Saleh, *Crystals*, 2023, **13**, 118; DOI: 10.3390/cryst13010118.
21. G. P. Zharkov, O. V. Filimonova, Yu. S. Petrova, A. V. Pestov, L. K. Neudachina, *Russ. Chem. Bull.*, 2022, **71**, 152; DOI: 10.1007/s11172-022-3389-2.
22. A. V. Pestov, E. V. Peresypkina, A. V. Virovets, N. V. Podberezskaya, Y. G. Yatluk, Y. A. Skorik, *Acta Crystallogr. C*, 2005, **61**, m510; DOI: 10.1107/s0108270105033780.
23. M. S. Bukharov, V. G. Shtyrlin, A. Sh. Mukhtarov, G. V. Mamin, S. Stapf, C. Mattea, A. A. Krutikov, A. N. Il´in, N. Yu. Serov, *Phys. Chem. Chem. Phys.*, 2014, **16**, 9411—9421; DOI: 10.1039/c4cp00255e.
24. L. G. Kuz´mina, A. V. Churakov, *Russ. Chem. Bull.*, 2022, **71**, 283; DOI: 10.1007/s11172-022-3409-2.
25. A. G. Medvedev, A. A. Mikhailov, P. V. Prikhodchenko, T. A. Tripol´skaya, O. Lev, A. V. Churakov, *Russ. Chem. Bull.*, 2013, **62**, 1871; DOI: 10.1007/s11172-013-0269-9.
26. N. Yu. Serov, A. V. Ermolaev, V. G. Shtyrlin, *27th Int. Chugaev Conf. on Coordination Chemistry (Nizhny Novgorod*, *October 2—6*, *2017)*, *Book of Abstracts*, Nizhny Novgorod, 2017, p. Y38.
27. N. Yu. Serov, V. G. Shtyrlin, M. S. Bukharov, A. V. Ermolaev, E. M. Gilyazetdinov, A. A. Rodionov, *Polyhedron*, 2021, **197**, 115041; DOI: 10.1016/j.poly.2021.115041.
28. N. Yu. Serov, V. G. Shtyrlin, M. S. Bukharov, A. V. Ermolaev, E. M. Gilyazetdnov, K. V. Urazaeva, A. A. Rodionov, *Polyhedro*n, 2022, **228**, 116176; DOI: 10.1016/j.poly.2022.116176.
29. R. R. Garipov, V. G. Shtyrlin, D. A. Safin, Yu. I. Zyavkina, F. D. Sokolov, A. L. Konkin, A. V. Aganov, A. V. Zakharov, *Chem. Phys.*, 2006, **320**, 59—74; DOI: 10.1016/j.chemphys.2005.06.026.
30. S. Stoll, A. Schweiger, *J. Magn. Reson.*, 2006, **178**, 42—55; DOI: 10.1016/j.jmr.2005.08.013.
31. I. I. Mirzayanov, A. R. Garifzyanov, D. R. Islamov, V. G. Shtyrlin, *Russ. J. Gen. Chem.*, 2020, **90**, 381—384; DOI: 10.1134/S1070363220030081.
32. M. S. Bukharov, E. M. Gilyazetdinov, N. Yu. Serov, A. I. Gizatullin, A. V. Ermolaev, N. S. Aksenin, A. R. Garifzyanov, I. I. Mirzayanov, D. R. Islamov, V. G. Shtyrlin, *Sb. materialov XIV Vseross. molodezhnoi nauchno-innovatsionnoi shkoly "Matematika i matematicheskoe modelirovanie"* [*Collection of Materials of the XIV All-Russian Youth Scientific and Innovative School "Mathematics and Mathematical Modeling"*] *(Sarov, April 7—9, 2020)*, Sarov, Interkontakt, 2020, pp. 15—16 (in Russian).
33. N. V. Shtyrlin, R. M. Khaziev, V. G. Shtyrlin, E. M. Gilyazetdinov, M. N. Agafonova, T. I. Vinogradova, M. Z. Dogonadze, N. V. Zabolotnykh, E. G. Sokolovich, P. K. Yablonskiy, Y. G. Shtyrlin, *Med. Chem. Res.*, 2021, **30**, 952—964; DOI: 10.1007/s00044-021-02705-w.

Received November 23, 2022;
in revised form January 13, 2023;
accepted January 23, 2023